Calculating Time-Resolved Absolute Number Densities of Reactive Species via Cavity Ringdown Spectroscopy

Undergraduate Research Thesis

Presented in Partial Fulfillment of the Requirements for graduation "with Honors Research Distinction in Chemistry" in the College of Arts and Sciences of The Ohio State University

By

Ian W. Jones,

Undergraduate Program in Chemistry

The Ohio State University

2021

Thesis Committee:

Professor Terry A. Miller, Department of Chemistry and Biochemistry, Advisor

Professor James Coe, Department of Chemistry and Biochemistry

Professor Igor Adamovich, Department of Mechanical and Aerospace Engineering

Abstract:

To test proposed kinetic mechanisms, the measurement of absolute concentrations is important and often required. Numerous spectroscopic techniques have been used to follow the concentration of reactive species, such as radicals or excited states, throughout processes like chemical reactions or relaxations to the ground state. However, highly reactive states are difficult to measure absolute populations for. To obtain quantitative values for these populations, cavity ringdown spectroscopy experiments were performed by the Adamovich group. In conjunction with this experimental work, a series of calculations were performed to calculate the absolute populations of two species: metastable N_2 and HO_2 radical. To perform these calculations, a series of constants and parameters from prior experiments were used to form a simulation on the program Pgopher, which generated values used to calculate the absolute cross-sections required to convert the experimentally obtained absorption coefficients into absolute number densities. In the metastable N_2 experiment and calculations, the absolute cross-sections were calculated using two different methods using values obtained from prior experiments before they were converted into number densities. In the HO_2 experiment, the absolute cross-sections were instead determined by first fitting the dipole moments of a simulated spectrum to a set of empirical cross-sections from a prior experiment, then changing the conditions of the simulation to match those of the corresponding experiment, yielding a spectrum whose peaks were cross-sections that enabled number densities to be obtained from the observed absorption coefficients.

Table of Contents:

Section I: Introduction

Absolute populations refer to the number of molecules in a given quantum state and can be summed over all quantum states. They are often expressed as a concentration, using units such as molecules*cm^{-3}. These values are critical to analytical chemistry as the resulting concentrations of an excited molecule or product are important in determining both the effectiveness and the efficiency of a process, as well as in quantifying the amount of a specific substance present in a sample. The ease of measurement of the absolute populations of different substances vary. Reactive species such as radicals or metastable/unstable states are particularly difficult to extract absolute populations from due to their short lifetimes and sensitivities to interferences from common molecules such as water. The reactive nature of these molecules, while increasing the difficulty of taking measurements, also increases the importance of measuring absolute populations of these molecules, as these more reactive molecules are important to track due to the radical reactions that they readily undergo. In analyzing these molecules, it is essential that the methods that are utilized are both sensitive enough to detect the molecules and selective enough to avoid any interference or noise from molecules other than the target molecule. While most types of spectroscopy are sensitive, the only type of spectroscopy that directly provides data that can be used to get quantitative values for populations is absorption spectroscopy. However, since most absorption experiments involve analyzing the intensity of incident light as a function of wavelength, and the amount of light absorbed by the target molecules tends to be small, most absorption spectroscopy methods are not sensitive, because the differences in intensity are small in relation to the both the initial and final intensities [1]. This issue is resolved by utilizing a specific method of absorption spectroscopy known as Cavity Ringdown Spectroscopy (CRDS).

Absorption experiments operate based on the Beer-Lambert Law

$$I = I_0 * \exp(\sigma N L) \quad (1),$$

where σ is the absorption cross-section at a given wavelength, N is the difference in number density between the initial and final state of the absorbing species, and L is the absorption path length of the absorbing medium. The value of σNL is very small in the

majority of absorption experiments, which leads to the small difference in intensity between I and I_0. Cavity ringdown spectroscopy addresses this problem through the absorption path length. Cavity ringdown spectroscopy operates by trapping photons from short pulses of laser light in a cavity with two opposite facing mirrors with a reflectivity of over 99.99%. Incident light that passes through the first mirror will rebound between the two mirrors repeatedly for an extended distance (typically around 10^4-10^5 passes) while a small fraction of the photons in the cavity leak through the opposite end with each cycle (this number decreases exponentially with each cycle for which the photons are present in the cavity) [1]. This drastic increase to the absorption path length greatly increases the difference between the initial and final intensities in the above Beer-Lambert Law, which corresponds to a significant increase in sensitivity.

There are multiple experiments that utilize CRDS to determine the absolute number densities of reactive states or molecules. Of these experiments, the two that will be receiving attention here are the use of CRDS in determining the time-resolved number densities of multiple rotational states of N_2 in the electronically excited metastable state of $N_2(A^3\Sigma_u^+)$ and from them the vibrational state populations using a Boltzmann distribution for the rotational levels [2] as well as the use of CRDS to determine absolute, time-resolved number densities for HO_2 in dilute fuel-O_2-Ar mixture excited by a plasma pulse in a heated plasma flow reactor under heat [3]. These experiments were performed alongside a series of calculations and simulations in order to independently calculate the absolute number densities of these reactive molecules by different means and to then compare the results of these different methods. This research was a collaborative effort between two groups: the Miller group and the Adamovich group. The Adamovich group performed all experimental work as well as some of the calculations below. The Miller group, whose results are the main focus of this work, were in charge of the accompanying calculations used to determine the values of the absolute cross-sections and number densities. The majority of these calculations were performed using the program Pgopher [4].

Section II: A Brief Overview of the Spectroscopic Method and its Requirements

Section IIA: Assigning Observed Transitions

Pgopher is a general purpose program formed from the merger of previous programs constructed to simulate and fit rotational, vibrational, and electronic spectra. The program is operated through a series of different windows wherein the target spectrum can be altered or its results examined. The main window of Pgopher is the graph showing the spectrum that is being simulated. Simulations can be added or edited in the Constants window, which contains all of the options to determine the geometry of the molecule as well as the cells to introduce, alter, or fit the molecular constants or transition moments of a molecule. Once a simulation is formed, the individual transitions of the molecule can be selected by right clicking them on the spectrum and opening the Linelist window, the window wherein assignments are made and frequency fits are performed. The individual transitions can also be selected for in the Transition window and other information such as the eigenvalues, eigenvectors, partition function, etc. can be found in various other windows within Pgopher.

One of these windows, the Overlay window, is of particular interest when working with experimental data or linelists. Using the Overlay window, the program Pgopher can take a list of assigned lines and perform least squares fits to alter any number of floated constants to determine the best values of said constants. Under a circumstance where the determination of these constants is done from scratch, the assignment of lines would require a series of estimates of first lower, then higher order, constants, each accompanied by an iterative fitting process, until a simulation that fits broad sections of the spectrum is developed. However, both the metastable N_2 band and the overtone of the HO_2 band have been examined in previous studies which have developed both linelists and sets of molecular constants, allowing the assignment of lines to be performed by comparing the lines on the linelist to the spectrum developed by the molecular constants given to Pgopher.

Section 2B: Relating Observed Intensities to Concentrations

The experiments in which both the metastable N_2 and the HO_2 radical were examined were performed using CRDS, which provides the transmitted intensity from the laser light source defined [1,2] by

$$I(t) = I_0 \exp\left(-\frac{ct(1-R)}{L_{cell}}\right) \qquad (2),$$

where the emitted intensity I(t) is determined by the incident intensity (I_0), the speed of light (c), the time (t), the reflectivity of the mirrors (R), and the cavity length (L_{cell}). The addition of an absorbing species to the cavity changes [1,2] this equation to

$$I(t,v) = I_0 \exp\left(-\frac{ct(1-R)}{L_{cell}}\right) \exp\left(-\frac{ct\alpha(v)L_{abs}}{L_{cell}}\right) \qquad (3),$$

where $\alpha(v)$ refers to the molecular absorption coefficient as a function of the laser frequency, v, and L_{abs} the absorption path length. The validity of this equation requires that the laser light source emits over a narrow linewidth (compared to the molecular absorption) that resonates with a weak absorption transition of the species. In the particular study of metastable N_2 that these calculations accompanied, the normal conditions of narrow linewidth and weak absorption were not met, which required the individual cavity modes, m, to be summed to convert [2] from the above equation to

$$\frac{I(t)}{I_0} = \exp\left(-\frac{ct(1-R)}{L_{cell}}\right) \sum_m g_S(\nu_0-\nu_m) \exp\left(-\frac{ctg_A(\nu_0-\nu_m)\alpha L_{abs}}{L_{cell}}\right) \qquad (4),$$

where α refers to the line-integrated absorption coefficient (cm^{-1}*Hz) such that $\alpha(v) = g_A(v)\cdot\alpha$ [2]. The resulting sum extends to for all of the overlapping cavity modes within the absorption line. The value of the line-integrated absorption coefficient, α, was obtained from the above equation by matching the ring down decay signal I(t) to the experimental signal. The calculated absorption coefficient can be used to determine the absolute population of a given vibrational rotation state of an absorbing species through the equation [5]

$$N(v'',\gamma'') = \frac{\alpha}{k_{v_0}} = N(v'')f_{\gamma''}^{v''} \qquad (5),$$

where $N(v'', \gamma'')$ is the absolute population of an absorbing species with vibrational state v'' and rotational state γ'' (cm^{-3}) and k_{v_0} is the line-integrated cross-section (cm^2Hz). To The line-integrated cross-sections for metastable N_2 were calculated using the equation [6]

$$k_{v_0} = \frac{2\pi^2 v_0}{3\varepsilon_0 hc} \frac{S_{J',J''}}{2J''+1} \left| R_e^{v',v''} \right|^2 = \frac{2\pi^2 v_0}{3\varepsilon_0 hc} \frac{S_{J',J''}}{2J''+1} q_{v',v''} \left(R_e\left(\bar{r}_{v',v''}\right) \right)^2 \qquad (6),$$

where h is the Planck constant, c is the speed of light, ε_0 is the dielectric permittivity of vacuum, $q_{v',v''}$ is the Franck-Condon factor, and $R_e\left(\bar{r}_{v',v''}\right)$ is the electronic transition moment (both obtained from Ref. [7]). The cross-section was obtained using values for the electronic-vibrational transition moment $\left| R_e^{v',v''} \right|^2$ that were calculated in from the experimentally determined radiative lifetimes [7] and Honl London Factors $S_{J',J''}$ obtained from a Pgopher simulation, developed using molecular constants for the $B^3\Pi_g - A^3\Sigma_u^+$ from a previous study [8]. Assuming rotational-translational equilibrium, the fractional rotational population $f_{\gamma''}^{v''}$ is calculated using the equation [9]

$$f_{\gamma''}^{v''} = \frac{2\Phi hcB_{v''}}{3kT}(2J'' + 1) \exp\left(-\frac{E(\gamma'')hc}{kT}\right) \quad (7),$$

where Φ is the nuclear spin statistical weight factor ($\Phi = \frac{1}{3}$ $(even\ N'')$ or $\frac{2}{3}$ $(odd\ N'')$), which distinguishes between symmetric and antisymmetric rotational levels and $B_{v''}$ is the rotational constant of the v'' state [10].

Since the theory behind the equations listed above is applicable for any CRDS spectrum, the HO_2 absolute populations can be calculated using the same equations as the metastable N_2 absolute populations. However, the values of the cross-sections were obtained via a different method to that used for metastable N_2. Constants and a linelist from previous work [11] on a known concentration of HO_2 were used to simulate the frequencies of the transitions in the HO_2 spectrum. However, the pressure broadened linewidths and temperatures in the earlier work are different from those used in the present experiment, so the cross-sections can not be directly used. A Pgopher simulation of this medium was done with the molecular constnats from Ref. [12] and varying only the components of the transition moment along the a and b intertial axes. This fit was performed on multiple

small sections of the spectrum and the resulting transition moments and standard deviations in transition moment were compared and averaged using a weighted average based of the number of a and b component transitions present in each section of the spectrum. These new fitted intensities provided the peak cross-sections (in cm^2/molecule) to convert observed peak absorption values to the desired absolute populations. Once these fits were made, the linewidth and temperature conditions were then altered to those used in the Adamovich lab to calculate the new cross-sections [3].

The cross-sections for the first overtone transition of the O-H stretch of HO_2 are known from a previous experiment [11] (molecular constants from Ref. [12]). These cross-sections were done at a known linewidth and temperature as well as for a known concentration. Since the concentration was known, the cross-sections were obtainable by dividing the absorption coefficients by the concentrations. The conditions that were used in the previous experiment (T, linewidth) were used while a series of fits of small regions of the spectrum were performed.

Section III: Capabilities of Pgopher

Section IIIA: Formation of a Simulation

There are multiple values that must be filled in for a spectrum to appear on Pgopher [4]. The *New* option under the File dropdown contains a number of sets of molecular constants used as samples for different models used for the simulation (including linear molecules, symmetric and asymmetric tops, etc.) that have all the necessary values for a simulation to be created. When developing a simulation from scratch, the Constants window will contain only two sections, the section corresponding to the file, which will be named "." until a file name is saved, and the Simulation subsection under the File section. The File section contains multiple options that modify the data exported by Pgopher through either the Log Window or the *Export* option under file. Right-clicking the File section and highlighting the *Add New…* option provides several options for subsections to add, the most significant of which are the Simulation and Species subsections.

The Simulation subsection contains values that can be altered to modify both the spectrum itself and how the spectrum is presented. The upper list contains cells to alter the conditions the spectrum is taken under, including the temperature (in Kelvin) and the Gaussian and Lorentzian contributions to the lineshape. Additionally, the simulation window's dimension can be edited here. The x axis range that is displayed is determined by F_{min} and F_{max} and while the y axis range is determined by Y_{min} and Y_{max}. The number of points that appear on the simulation window is determined by the nDF value. The units of the x and y axes can also be determined in this section. The x axis units can be changed using the *PlotUnits* cell to a number of different units including cm^{-1} (denoted as cm1), Kelvin, eV, MHz, etc. The y axis units are changed via the *IntensityUnits* cell, and can be changed to various units of intensity, such as cm^2cm^{-1}permolec, nm^2MHzpermolec, arbitrary units, normalized units, etc., or PopDist or NormPopDist, which change the simulation to a linelist of the population distribution.

The other subsection, the Species subsection, contains only a few options to edit. The J_{min} and J_{max} values can be edited both here and in the inner subsections, but the cells here set the default maximum and minimum J values. In the simulations, the value used for J_{min} is -

0.5 (-1 for the metastable N_2), as the value instructs the simulation to use the lowest possible value of J for the minimum. Right-clicking on the Species header and selecting *Add New…* opens the options for the different models that can be used, including Linear, which was used for metastable N_2, and Asymmetric Top, which was used for HO_2. Selecting one of the models adds a molecule named after the type of model that was selected.

The Molecule subsection contains a different set of options depending on whether a linear or asymmetric top model was selected. Both simulations contain the *JAdjustSym* option, which determines whether the alternation of symmetry in J is accounted for. Changing the value of the cell does not change the simulation, but changes the notation for the peaks determined by the simulation. This value was changed to false for the simulation of metastable N_2, as the peaks of interest did not use rotationless parities. Additionally, the subsections for both models include the statistical weights, though the cells are different in correspondence to the difference between the models that are analyzed (*SymWt* and *AsymWt* for linear models and *eoWt*, *eeWt*, *ooWt*, and *oeWt* for asymmetric tops). The values here are held at 1 for HO_2, but the metastable $^{14}N_2$ has a *SymWt* of 2 and an *AsymWt* of 1. Since metastable N_2 has a center of symmetry, the value of *Symmetry* must also be set to true. The remainder of the settings in the Molecule section for the linear model pertain to the information given on the peaks in the Linelist section. The *ShowJ*, *ShowOmegaI*, *ShowN*, *ShowFNumber*, and *Showef* cells respectively show the upper and lower J, Ω, and N values, the f number of the transition, and the rotationless parity of the transition. The section for an asymmetric top contains a cell in which the point group (C_s in the case of HO_2) is entered. The molecule menu for an asymmetric top also contains two cells for setting up the axes of the simulation. The first of these cells in the *Representation* cell, which determines which of the inertial axes is mapped to which of the cartesian axes. In the case of HO_2, the Il representation is used. The axes are then mapped onto the molecule using the *C2zAxis* and *C2xAxis* cells. In the case of a C_s molecule, only the *C2zAxis* is set, as the only symmetry function is a plane of symmetry, which is mapped by setting the axis in *C2zAxis* to the inertial axis that lies perpendicular to the symmetry plane. For HO_2, the inertial axis set perpendicular to the C_s plane was the c axis. Right clicking this section and

selecting *Add New…* provides two subsections to add under the molecule which are both necessary for a simulation, the Manifold and Transition Moment subsections.

The Manifold subsection contains a few important settings. The *Initial* cell determines whether the population of any states within the manifold are used in calculating the partition function. This value must be set to True for at least one of the states used in the simulation in order for the simulation to run. Another setting, *AutoQConverge*, determines whether the value of Q is calculated until it converges or merely until the greatest value of J used for the calculation. This cell must be set to false for simulations that do not converge, or they will not load.

The subsection within this section is named Linear or Asymmetric Top for the two models and contains the majority of the cells in which the parameters of the simulation are entered. Alongside the parameters are several cells in the lower window which pertain to the state itself and differ between the linear and asymmetric top models. Both models include the *S* cell, in which the spin is entered (0.5 for HO_2 and 1 for metastable N_2). The State section for linear simulation also contains a cell to enter the electronic angular momentum (*Lambda*) and the *gerade* cell, where the state can be labeled gerade or ungerade. State subsections for asymmetric top molecules contain a cell labeled *Symmetry* in which the symmetry of the state is to be entered. The possible values depend on the point group, but for the band of HO_2 that was simulated, both the upper and the lower states have A' symmetry.

When a new transition moment is added, a window appears where the bra and ket are to be entered. There are no other significant settings to change in this section, as it serves to group together transition moments between states within the selected manifolds. Right-clicking on the section and highlighting *Add New*… provides potential transition moment types to add to the simulation including spherical transition moments (used for metastable N_2) and cartesian transition moments (used for HO_2). When a transition moment is selected, a window appears which again asks to select the states for the bra and ket of the dipole moment. The metastable N_2 simulation contains only a single dipole moment, but the HO_2 simulation contains a dipole moment that projects into two different axes,

simulated in Pgopher by two separate dipole moment components set to different axes. Within the section for a cartesian transition moment, the relative or absolute intensities of the dipole projection into different axes can be set using the *Strength* cell.

Section IIIB: Making of Frequency Assignments and Fits

In Pgopher, experimental spectra or linelists are added for comparison to the simulated spectrum using the overlay function. The overlay function contains several values that can be fitted to match the simulated spectrum to the simulation without changing the simulation itself. In addition to these settings, the is an option to distinguish the overlay as a linelist or a spectrum, which will consequently separate the points in the overlay into lines if selected. Once a line from the spectrum is identified, the matching line in Pgopher is assigned by finding it (either through the transition window or the main window), right clicking the line to add it to the Linelist window, clicking on the desired transition in the Linelist window, and then right clicking and dragging the cursor over the experimental line that the transition is to be matched to. This will change the frequency of the transition in the Pgopher linelist to the frequency of the selected observed line. Once a large subset of the observed lines has been assigned, a fit can be made by floating the target constants in the constants window, then selecting all of the target lines and subsequently selecting fit from the Linelist window. Once the calculation finishes, the constants in the window will have changed and will have the corresponding standard deviations of the results in the next column. The log window will also appear with a summary of the calculation that includes a standard deviation of all of the constants. Lastly, a window that shows the residuals of all of the observed transitions in comparison to the fitted results will appear. In order to obtain accurate results, it is recommended that the fit be performed 15 to 20 times or until the residual converges.

Section IIIC: Simulations and Fits using Intensities in Absolute Units

Pgopher simulations allow for a variety of different fits depending on the constants that are set to float and the fit type that is selected. Among the constants that can be floated are the components of the dipole moment of a transition. These can be fitted by a couple different methods. The first of these methods produces a fit similar to the least differences fit used to fit the molecular constants based on the frequencies of the transitions as described earlier. Similar to the previous fits, this method requires the selection of a series of lines from a linelist. In the Linelist Window, the advanced options contains a box labeled *Check I* that allows the intensities of transitions to be set to the values in a linelist alongside their corresponding frequencies. Similar to the frequency fits, this method requires a large number of lines to use effectively, and also requires the lines to be completely distinct from one another, which places limitations on its effectiveness, particularly when attempting to fit the transitions of HO_2, which frequently overlap and contain interferences that make fitting difficult. The other, more broadly applicable method is to perform a contour fit, which will fit the entire segment of the simulated spectrum which is contained within the screen to the overlay within the same section. To perform this fit, the transition moment components must be set to float similar to the other simulations. Additionally, the Overlay window must be opened and the header within corresponding to the overlay that the spectrum is to be fitted to must be highlighted. This is required as, in the instance that multiple overlays are present above the simulation, a single overlay must be selected to be fitted to. To select a narrow range and avoid interference from peaks not contained within both the simulation and the overlay, it is recommended that only the visible section of the spectrum be fitted (selected by right-clicking the overlay and choosing *Select Visible*). To perform the fit, open the log window, change the fit type in the dropdown in the top left corner to Contour, and fit the spectrum until the transition moments converge. The use of a small section for the fit limits the applicability of the fit to the entire spectrum, so contour fits that were performed were done in multiple sections of the spectrum to check for any inconsistencies in the projections of the transition moment. This method will not attempt to adjust the dipole moments to match the intensities of peaks not contained within the spectrum, and also generates a graph of the residual between the simulation and graph vs

the frequency at which that residual occurs. This graph is placed alongside the newly fitted simulation for comparison.

Section IV: Results

Section IVA: Metastable N_2 Results:

The electronically excited metastable state of N_2, $N_2(A^3\Sigma_u^+)$, is a significant factor in the kinetics of multiple setups, including electric discharge plasmas and high-temperature nonequilibrium reacting flows. Gas mixtures containing significant portions of nitrogen and air will produce a number of different excited states when exposed to an electric discharge. Of the different excited states that are produced, $N_2(A^3\Sigma_u^+)$ is one of the more common, as it is produced both directly by an impacting electron and via decay of higher energy states such as $N_2(B^3\Pi_g)$ [13]. In high-temperature setups wherein a hypersonic flow experiences shockwaves, $N_2(A^3\Sigma_u^+)$ may form through electron impact, heavy species impact, or N atom recombination [14]. Once excited, $N_2(A^3\Sigma_u^+)$ can be quenched via a collision by one of a number of different molecules including O_2, H_2, CH_4, C_2H_4, and C_2H_6. These collisions are an important source of several molecules in air and fuel-air mixtures including atomic oxygen and hydrogen as well as hydrocarbon radicals [15]. Additionally, $N_2(A^3\Sigma_u^+)$ plays an important role in low temperature air-plasmas and atmospheric pressure Ar plasma jets, in which its reactions with O_2 and O are major contributors to the formation of O and NO [16, 17].

The absolute populations of $N_2(A^3\Sigma_u^+)$ have long radiative lifetimes and relatively low number densities, which makes them difficult to quantify. Of the diagnostic techniques used recently to examine $N_2(A^3\Sigma_u^+)$, CRDS was among the most common as it provides direct measurements of the absorbing species' absolute number densities. In the experimental work, the absolute populations for multiple vibrational states were measured using a discharge of short pulses useful for generating time-resolved measurements of excited species and radicals.

The line integrated rotational cross-sections of multiple transitions identified both within the simulation generated by Pgopher and in the CRDS experiments are shown in the table below. The values for the Hönl-London Factor, rotational cross-section, fractional population, and vibrational cross-section were calculated via two different methods. Columns II, IV, VI, and VIII were determined directly from Pgopher while Column I was

obtained from a separate program and Columns III, V, and VII were calculated from other references as described in Section II and the postmarks to the table.

Table IVA.1: Hönl-London factors, rotational and vibrational cross-sections, and fractional populations of sample transitions from $N_2(A^3\Sigma_u^+, v=0\text{-}2)$ bands calculated by two methods

Transition Name and Wavelength	Hönl-London Factor, $S_{J',J''}$		Rotational Cross-section, k_{v0} (cm²·Hz)		Fractional Population, $f_{\gamma''}^{v''}$		Vibrational Cross-section, $A_{\gamma''}^{v''}$ (cm²·Hz)	
	I[a]	II[b]	III[c]	IV[b]	V[d]	VI[b]	VII[e]	VIII[b]
$v''=0$, $R_{11}(20)$, N"=19, J"=20, λ_0(nm)=766.854	18.7	18.7	$4.67\cdot10^{-6}$	$4.74\cdot10^{-6}$	$8.81\cdot10^{-3}$	$8.80\cdot10^{-3}$	$4.12\cdot10^{-8}$	$4.17\cdot10^{-8}$
$v''=1$, ${}^{S}R_{32}(12)$, N"=12, J"=12, λ_0(nm)= 753.646	3.65	3.78	$2.58\cdot10^{-6}$	$2.69\cdot10^{-6}$	$1.30\cdot10^{-2}$	$1.31\cdot10^{-2}$	$3.37\cdot10^{-8}$	$3.51\cdot10^{-8}$
$v''=2$,${}^{N}P_{13}(6)$, N"=7, J"=6, λ_0(nm)= 752.721	0.70	0.56	$9.80\cdot10^{-7}$	$8.08\cdot10^{-7}$	$2.75\cdot10^{-2}$	$2.69\cdot10^{-2}$	$2.69\cdot10^{-8}$	$2.17\cdot10^{-8}$
$v''=0$, $Q_{11}(12)$, N"=11, J"=12, λ_0(nm)=773.215	18.2	18.0	$7.40\cdot10^{-6}$	$7.40\cdot10^{-6}$	$3.09\cdot10^{-2}$	$3.08\cdot10^{-2}$	$2.29\cdot10^{-7}$	$2.27\cdot10^{-7}$
$v''=1$,${}^{O}P_{12}(12)$, N"=12, J"=12, λ_0(nm)=764.638	3.75	3.93	$2.61\cdot10^{-6}$	$2.75\cdot10^{-6}$	$1.30\cdot10^{-2}$	$1.31\cdot10^{-2}$	$3.39\cdot10^{-8}$	$3.60\cdot10^{-8}$

[a] From program in Ref. [9]

[b] From pGopher program [4]

[c] From column I and Eq. (6)

[d] From Ref. [5], Eq. (7)

[e] Product of Columns III and V

The two programs that were used to separately determine the Hönl-London Factor had good agreement, with the only significant disparity came from the v"=2 transition at λ_0= 752.721 nm, the others falling within 10% of one another. The rotational cross-sections saw a similar level of agreement. The fractional populations, which was both calculated using Equation 7 [5] and obtained from the Pgopher normalized population distribution linelist, all had good agreement, including the v"=2 transition at λ_0= 752.721 nm, which fell within 10% difference. The vibrational cross-sections, which are calculated from the previous values using similar methods both for the calculations listed above and in Pgopher, also mostly had good agreement.

Once the values for the vibrational cross-sections were determined, the absorption coefficient, which was obtained experimentally for multiple transitions, as can be seen in Graph IVA.1 below. The values of the absorption coefficient for the individual transitions were then used to convert the cross-sections to the absolute number densities listed below. The uncertainties in the number densities listed were based on the standard deviation of the line-integrated absorption coefficient as the laser scanned across the line, with an average of 15 laser shots was used for the calculation for an individual point in the line.

Graph IVA.1: Spectral traces comparing the convolution of the Lorenzian profile of the laser line shape and the Voigt profile of the absorption line shape with the experimental absorption line shape at P = 22 Torr

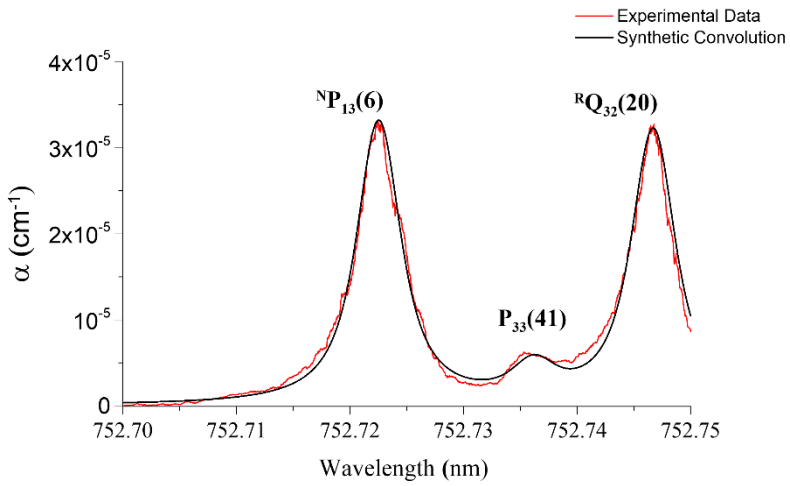

Table IVA.2: Absorption coefficients and absolute peak populations of sample transitions from $N_2(A^3\Sigma_u^+, v=0\text{-}2)$ bands

Transition	Absorption Coefficient, α ($cm^{-1}\cdot Hz$)	$N(v'', \gamma'')$ (cm^{-3})	$N(v'')$ (cm^{-3})
$v''=0$, $R_{11}(20)$, N"=19, J"=20, λ_0 (nm) = 766.854	$1.04\cdot10^{5}$	$(2.20\pm0.72)\cdot10^{10}$	$(2.51\pm0.82)\cdot10^{12}$
$v''=1$, ${}^{S}R_{32}(12)$, N"=12, J"=12, λ_0 (nm)= 753.646	$1.47\cdot10^{5}$	$(5.45\pm3.04)\cdot10^{10}$	$(4.18\pm2.32)\cdot10^{12}$
$v''=2$, ${}^{N}P_{13}(6)$, N"=7, J"=6, λ_0 (nm) = 752.721	$4.74\cdot10^{4}$	$(5.87\pm1.94)\cdot10^{10}$	$(2.18\pm0.72)\cdot10^{12}$
$v''=0$, $Q_{11}(12)$, N"=11, J"=12, λ_0 (nm) = 773.215	$1.50\cdot10^{6}$	$(2.03\pm0.20)\cdot10^{11}$	$(6.61\pm0.66)\cdot10^{12}$
$v''=1$, ${}^{O}P_{12}(12)$, N"=12, J"=12, λ_0 (nm) = 764.638	$1.09\cdot10^{6}$	$(4.96\pm0.62)\cdot10^{11}$	$(3.02\pm0.47)\cdot10^{13}$

From the values of the absorption coefficient obtained from traces such as Graph IVA.1, the time-resolved populations of $N_2A^3\Sigma_u^+$ can be tracked. To generate graphs detailing the time-dependence of the concentration of the excited electronic state, a single discharge or

burst of multiple pulses was fired and a series of CRDS scans of the spectrum were taken in the following milliseconds. These scans, which all appear similar to Graph IVA.1, each represent an individual value of the number density shown on the time-resolved graph. In both the single pulses and group of 5 pulses, the sharp decline after the pulse appeared to be exponential, indicating that the rate of decay was likely pseudo-first order.

Section IVB: HO_2 Overtone Band Results:

Hydroperoxy radical, or HO_2, is a prominent radical species that persists in low-temperature plasmachemical oxidations of both hydrogens and hydrocarbons [18]. Due to the role that HO_2 plays in the kinetics of the combustion and the fuel it can reform when used in plasma-excited fuel-oxidizer mixtures, obtaining number densities are essential to quantifying its role. In H_2 air mixtures, the mixture of primary focus in this report, H atoms generated by the electron impact dissociation of H_2 or energy transfer from excited N_2 will quickly generate HO_2 by combination with oxygen gas. Increasing the temperature of the system will result in the propagation of the chain, which leads to the chain branching and ignition of the mixture [19, 20]. Determining a balance at which the radicals will recombine while the chain propagates is difficult. The balance is quantified by obtaining absolute, time-resolved, in situ HO_2 concentrations under specified conditions. As was the case in Section IVA, the necessity of obtaining absolute number densities lends itself to the use of CRDS, as it provides direct measurements of the cross-sections to make these calculations.

Graphs IVB.1-IVB.7 and the corresponding Table IVB.1 below show the contour fits performed on small segments of the spectrum previously observed [11] of HO_2 of a known concentration that determined values for the dipole moment projections along both the a and b inertial axes and the standard deviation in these values. The first row, the calculated values for the dipole moment, were obtained from an ab initio calculation performed by the Stanton group in collaboration with this work. For each of the sections of the spectrum, the number of both a and b peaks present is included, and the weighted averages for the dipole moment projections and their standard deviations is weighted based of the number of peaks within each spectrum of the spectrum that correspond to transitions in the a and b inertial axes. In the graphs of the different segments of the spectra shown below, there are

two graphs aligned horizontally with one another. The upper member of each pair of graphs shows the intensity residuals by the frequency. The lower graph has two traces, where the maroon trace shows the experimental spectrum that was added as an overlay while the black trace shows the Pgopher simulation. While the residuals in the graphs are generally low, there are multiple sections where the lineshape formed is a sharp positive peak followed by a sharp negative peak or vice versa. These high residuals are a result of slight misalignments in frequency predicted by the simulation and experiment. This error is the result of slight perturbations of the spectrum within the given region due to the influence of vibrational levels that were not included in the calculation.

The value of the dipole moment projection along the a axis is relatively consistent across the spectrum, and many of the fitted values are relatively close to both the average dipole moment projection and the dipole moment projections from the ab initio calculations. Additionally, the standard deviations in the fitted dipole for this axis were relatively low, impacting mostly the third significant figure. In contrast, the fitted dipole moment for the b axis changed substantially with each segment of the spectrum, ranging from -0.0124 to -0.0173 Debye. This variance is reflected in the standard deviations of the different segments as well, as many of the standard deviations were multiple times larger than their a axis counterpart (most notably in Segment 4, where the difference is an entire order of magnitude). The cause of this disparity in fit quality likely stems from the number of peaks present along the a axis in comparison to the b axis. The b axis had far fewer peaks than the a axis in most of the segments. The segments with the most b peaks also tended to have lower standard deviations (though none as low as the standard deviations in the a projection).

Graph IVB.1: Comparison between experimental spectrum from a previous work (maroon) and Pgopher simulation (black) and intensity residuals (top) from 6631.0-6632.5 cm^{-1}

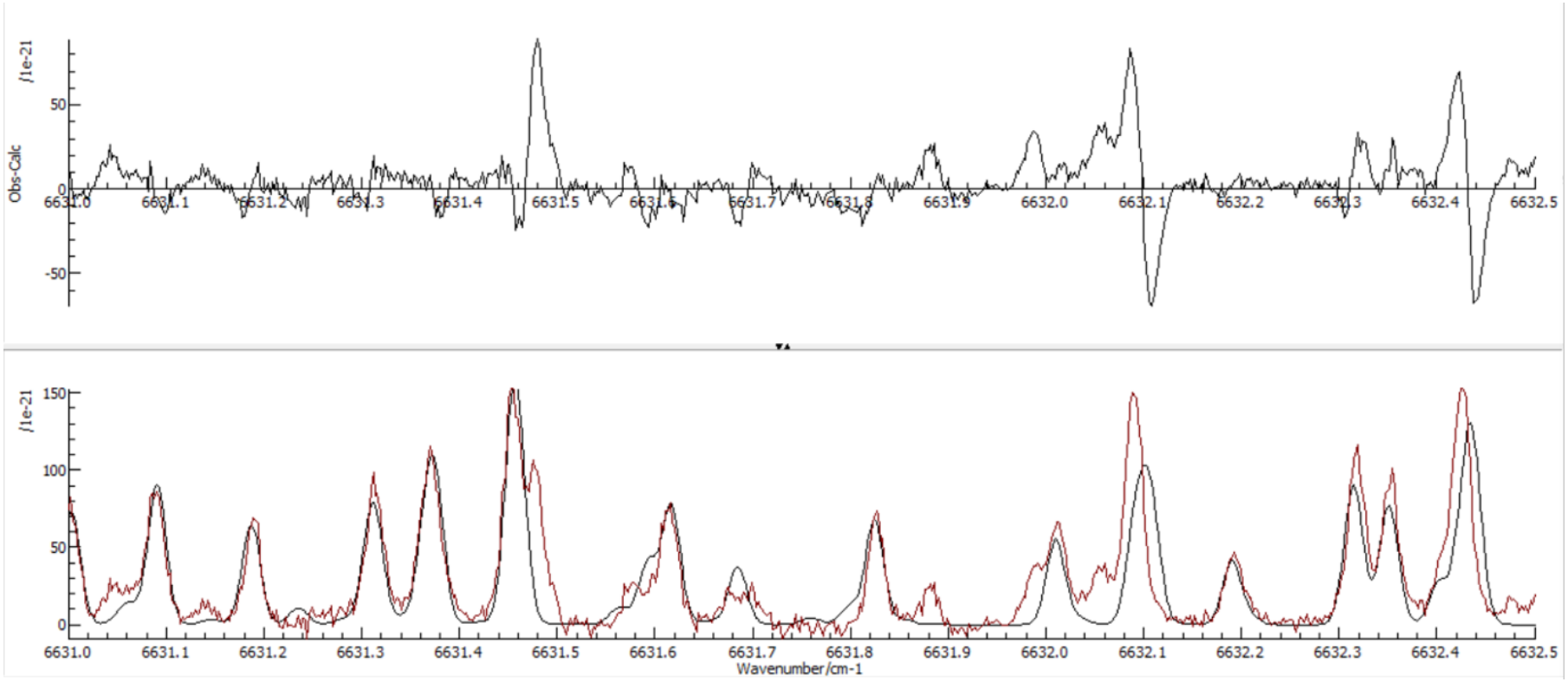

Graph IVB.2: Comparison between experimental spectrum from a previous work (maroon) and Pgopher simulation (black) and intensity residuals (top) from 6655.0-6656.5 cm^{-1}

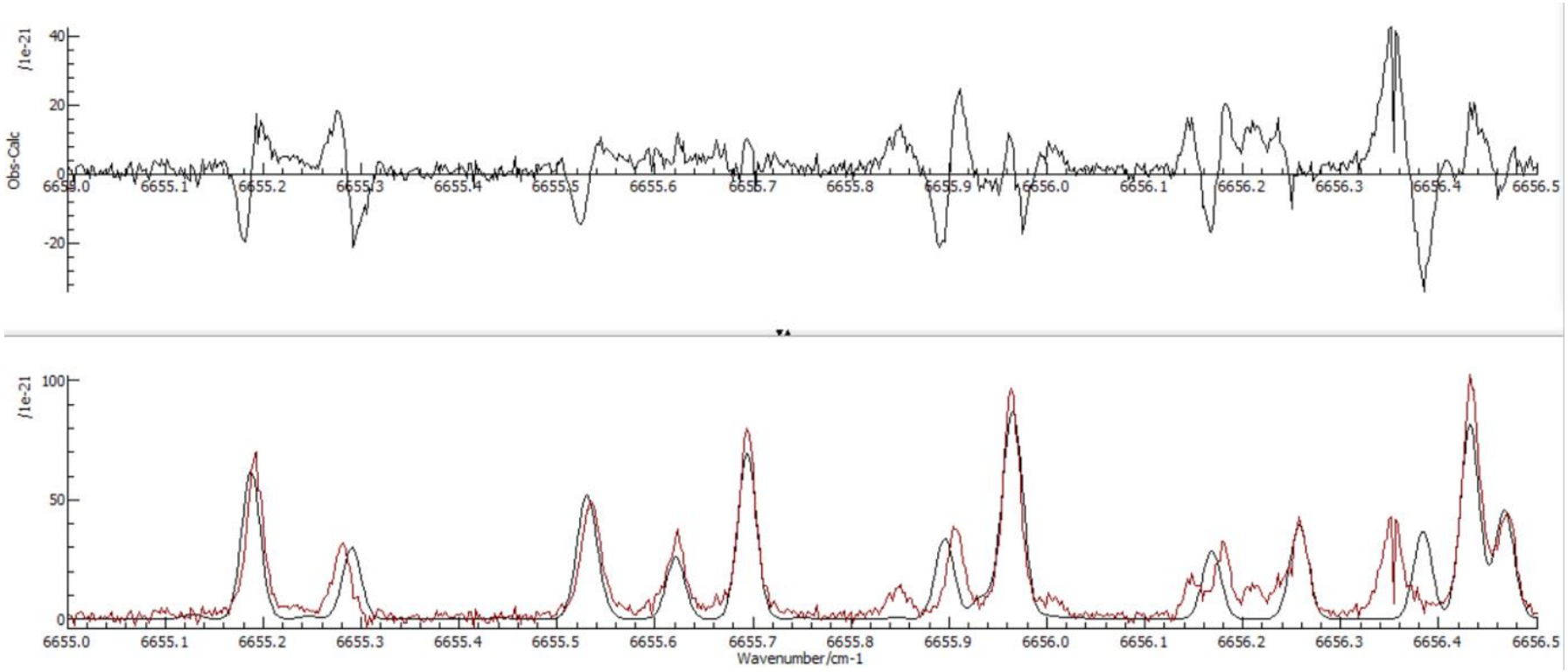

Graph IVB.3: Comparison between experimental spectrum from a previous work (maroon) and Pgopher simulation (black) and intensity residuals (top) from 6656.5-6658.0 cm^{-1}

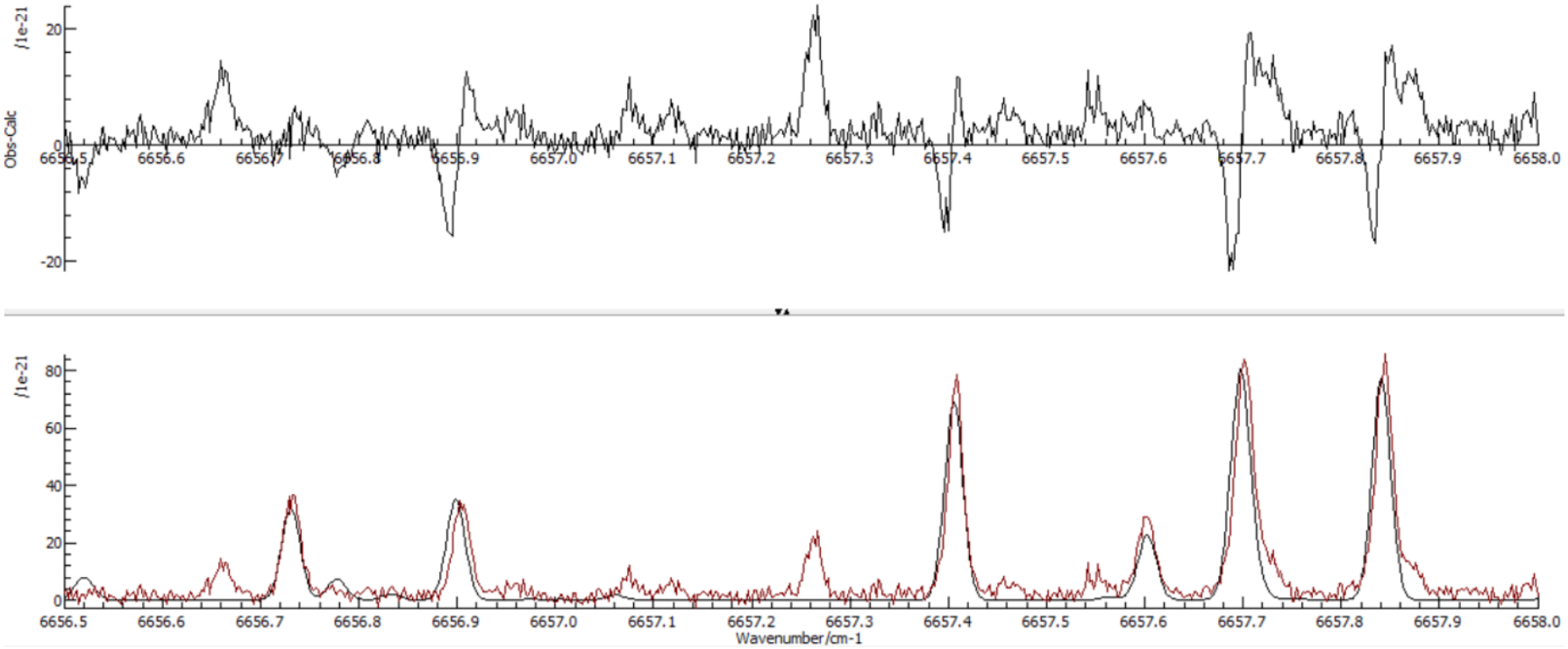

Graph IVB.4: Comparison between experimental spectrum from a previous work (maroon) and Pgopher simulation (black) and intensity residuals (top) from 6661.6-6663.1 cm^{-1}

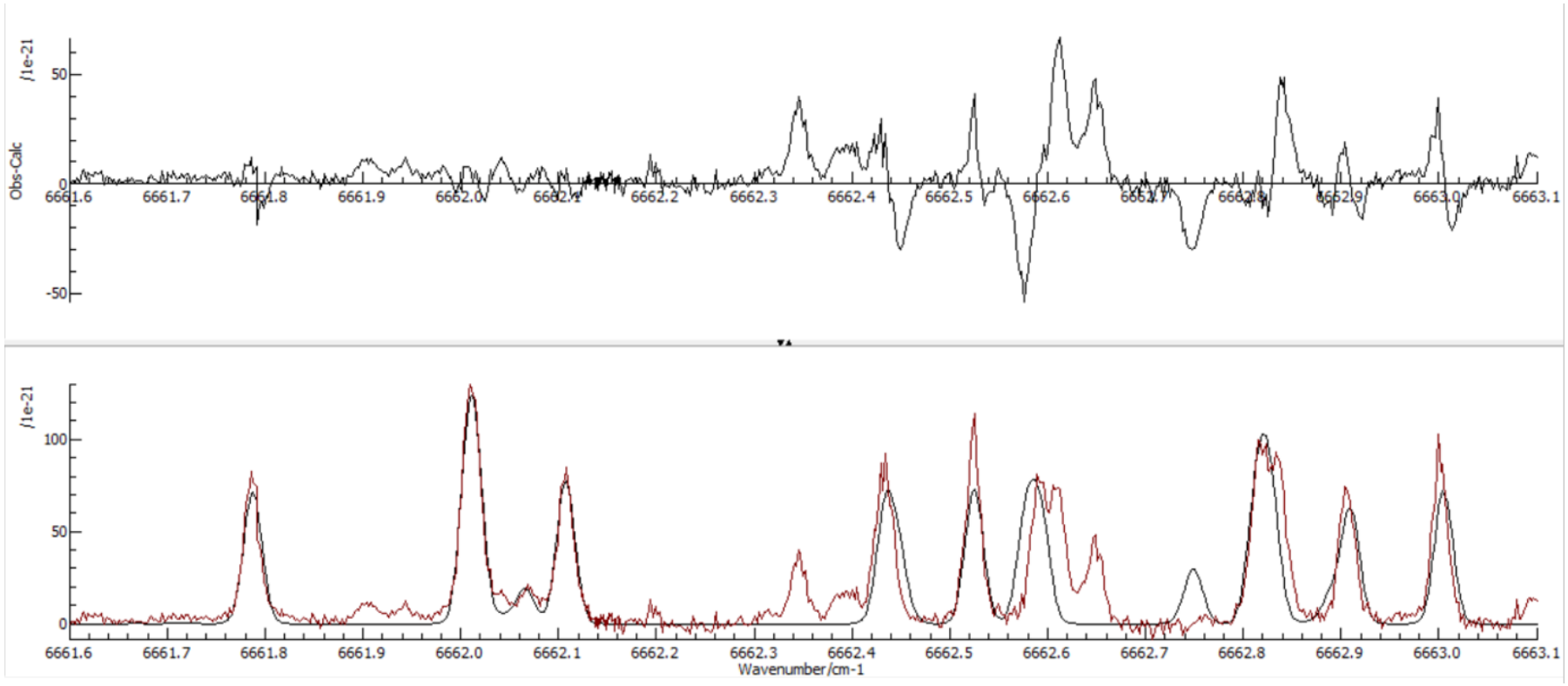

Graph IVB.5: Comparison between experimental spectrum from a previous work (maroon) and Pgopher simulation (black) and intensity residuals (top) from 6634.2-6634.8 cm^{-1}

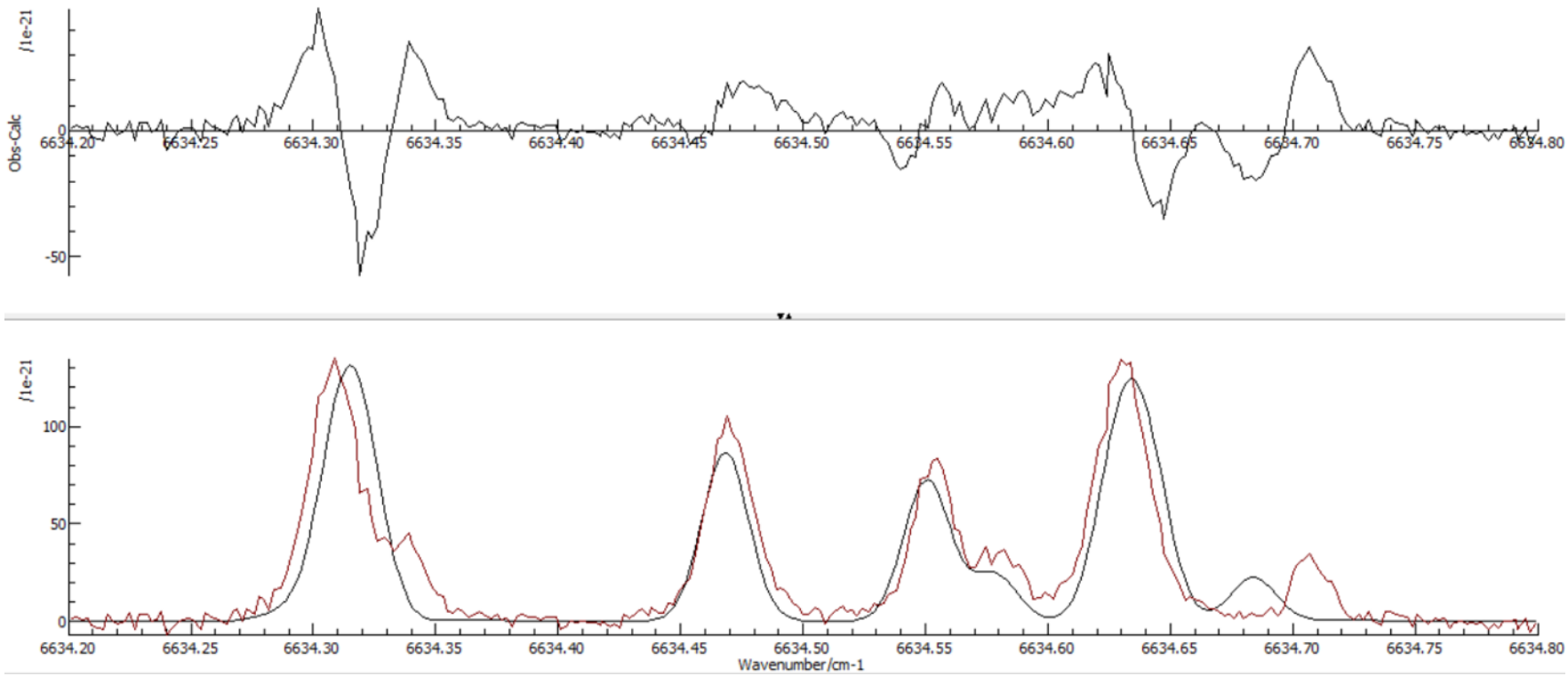

Graph IVB.6: Comparison between experimental spectrum from a previous work (maroon) and Pgopher simulation (black) and intensity residuals (top) from 6645.0-6645.8 cm^{-1}

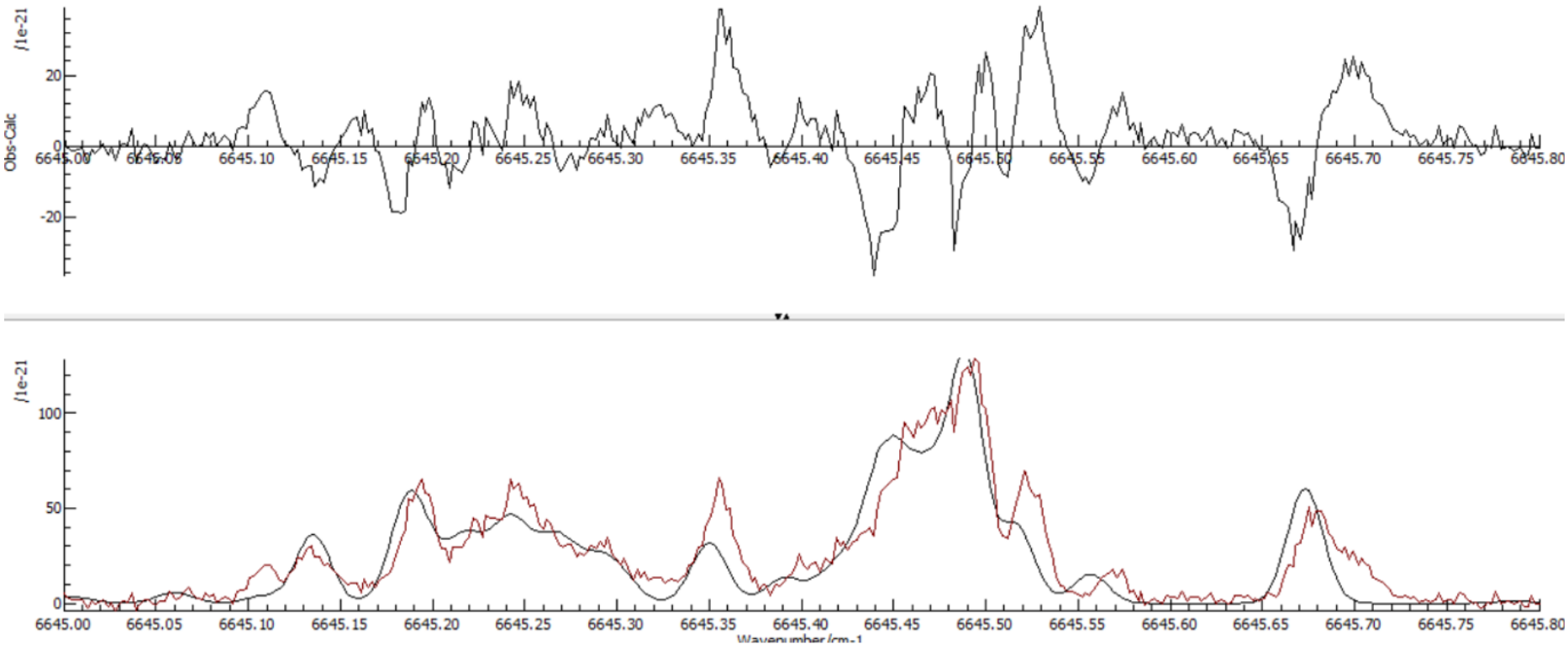

Graph IVB.7: Comparison between experimental spectrum from a previous work (maroon) and Pgopher simulation (black) and intensity residuals (top) from 6628.45-6629.70 cm^{-1}

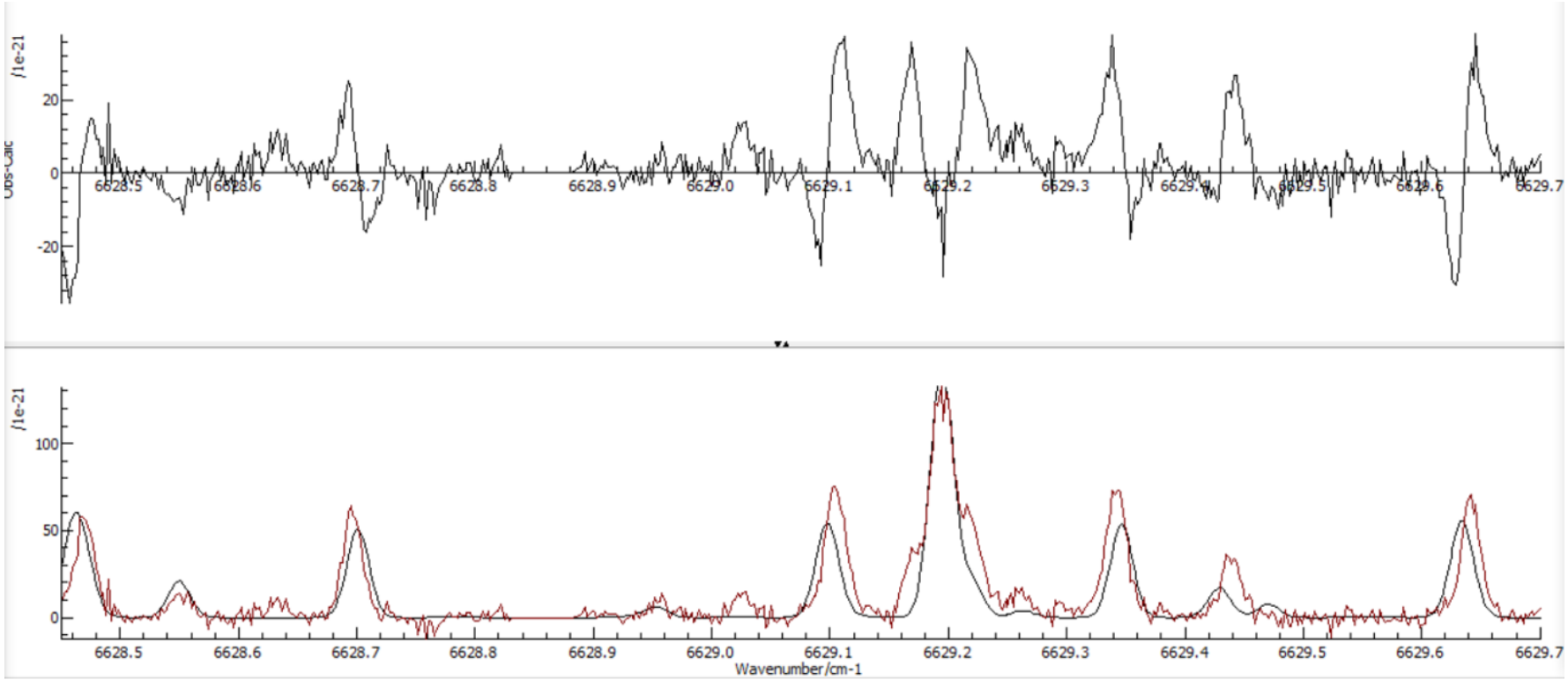

Note: Peak between 6628.8 and 6628.9 zeroed out for this contour fit

Table IVB.1: Contour fit ranges, the resulting dipole moments, the standard deviation in the fitted dipole moments, and number of a and b transitions within the fit range

Simulation	Fit Range (cm^{-1})	a DPM (Debye)	b DPM (Debye)	a Stdev	b Stdev	a/b peak count
Calculated Values	-	0.01485786	-0.015666187	-	-	-
1	6631.0-6632.5	0.015259338	-0.016627387	0.00019	0.00023	5, 12
2	6655.0-6656.5	0.015216115	-0.015110956	0.00012	0.00053	10, 2
3	6656.5-6658.0	0.015511333	-0.013925539	0.00012	0.00027	3, 5
4	6661.6-6663.1	0.015354337	-0.017311392	0.00015	0.00152	10, 3
5	6634.2-6634.8	0.016135087	-0.012498383	0.00018	0.00095	4, 2
6	6645.0-6645.8	0.014808478	-0.017392618	0.00017	0.00041	12, 4
7	6628.45-6629.7	0.014531143	-0.012946623	0.00018	0.00020	3, 8
Average (Weighted)	-	0.015199377	-0.015262574	0.000156	0.000413	-
Average (Unweighted)	-	0.015259404	-0.015116128	0.000159	0.000587	-

Similarly to in Section IVA, the values of the absorption coefficient that were obtained from the spectral trace (this time represented in Graph IVB.8, which has the trace at multiple different temperatures) were used to calculate number densities. These individual traces were taken in vast numbers in the brief period of time when the number densities experienced a sharp decline. Each of the individual traces is a single point on Graph IVB.9.

Graph IVB.8: Spectral absorption coefficient in a 2% H_2 – 2% O_2 – 96% Ar mixture 100 microseconds after the discharge at varying temperatures and P = 130 torr

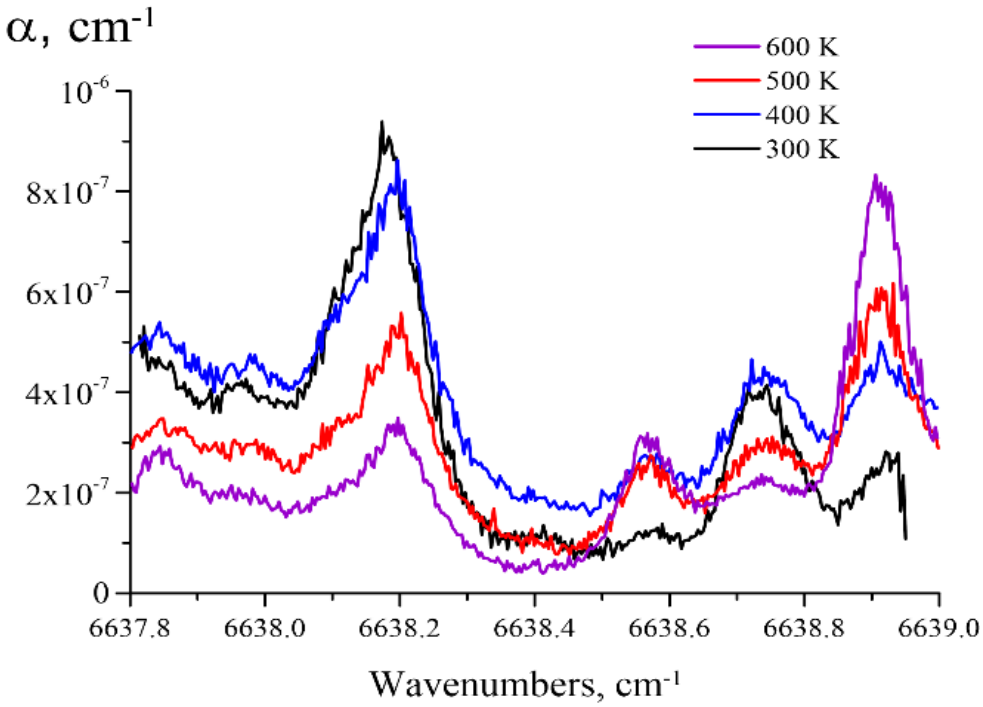

Graph IVB.9: Experimental time-resolved absolute number densities of HO_2

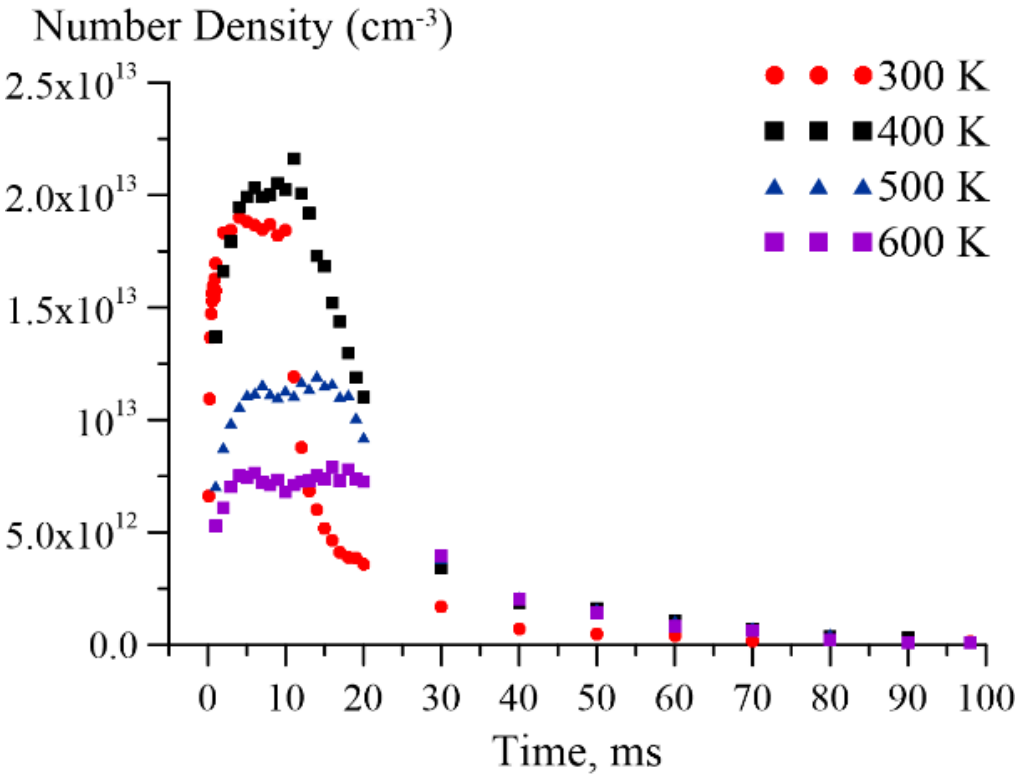

Section V: Conclusion

A method through which the absolute populations of reactive molecules or states of molecules can be calculated has been developed. Through both simulations in Pgopher and calculations, the absolute cross-sections of multiple states of metastable N_2 and HO_2 radical were calculated. In the instance of metastable N_2, calculations of the cross-section were performed using both previously derived constants and equations and through the use of Pgopher to calculate the Hönl-London factors, cross-sections, and fractional populations. The two methods yielded results that had good agreement, and the resulting absolute cross-sections were used to determine the absolute populations of metastable N_2 to generate a plot of its time dependence. For the HO_2 work, a set of empirical cross-sections were available under given conditions of pressure and temperature. The peaks within the spectrum were simulated by Pgopher by fitting to the cross-sections using a series of fits of small sections of the spectrum, from which the two transition dipole moment components were determined. The parameters of Pgopher were then changed to match the conditions of the present experiment, and the resulting peak intensities provided the values of the absolute cross-section to determine the absolute populations. The general theory behind the method holds for most CRDS experiments and going forward the next experiment will be to test more complex molecules with more sources of interference. In particular, the T and G conformers of both ethyl peroxy ($C_2H_5O_2$) and its deuterated form ($C_2D_5O_2$) will be analyzed to obtain their transition dipole components, which then can be used to determine populations.

Works Cited:

1. Chen, M. “Laser Spectroscopy Studying Organic and Inorganic Intermediates in the Atmospheric Oxidation Process”, Dissertation, The Ohio State University, 2011.
2. E.R. Jans, K. Frederickson, T.A. Miller, I.V. Adamovich, Time-resolved populations of $N_2(A^3\Sigma_u^+,v)$ in nanosecond pulse discharge plasmas, *Journal of Molecular Spectroscopy*, Volume 365, 2019.
3. E.R. Jans, X. Yang, I. W. Jones, T.A. Miller and I. V. Adamovich. "Measurements of HO2 Radical in a Preheated Plasma Flow Reactor," AIAA 2021-1144. *AIAA Scitech 2021 Forum*. January 2021.
4. PGOPHER, A Program for Simulating Rotational, Vibrational and Electronic Spectra, C. M. Western, *Journal of Quantitative Spectroscopy and Radiative Transfer*, 186 (2016) 221
5. Foissac, C., A. Campargue, A. Kachanov, P. Supiot, G. Weirauch, and N. Sadeghi, “Intracavity laser absorption spectroscopy applied to measure the absolute density and temperature of $N_2(A^3\Sigma_u^+)$ metastable molecules in a flowing N_2 microwave discharge”, *J. Phys. D: Appl. Phys.* 33 (2000) 2434
6. A.P. Yalin and R.N. Zare, “Effect of laser lineshape on the quantitative analysis of cavity ring-down signals”, *Laser Phys.* 12 (2002) 1065
7. F.R. Gilmore, R.R. Laher, and P.J. Espy, “Franck–Condon Factors, *r*-Centroids, Electronic Transition Moments, and Einstein Coefficients for Many Nitrogen and Oxygen Band Systems”, *J. Phys. Chem. Ref. Dat*a 21 (1992) 1005
8. C. M. Western, L. Carter-Blatchford, P. Crozet, A. J. Ross, J. Morville and D. Tokaryk, “The spectrum of N_2 from 4500 to 15700 cm^{-1} revisited with PGOPHER", *J. Quantitative Spectroscopy and Radiative Transfer* 219 (2018) 127
9. E.E. Whiting, “Computer program for determining rotational line intensity factors for diatomic molecules,” NASA Ames Research Center, Moffett Field, CA, Technical Note TN D-7268, Sept. 1973
10. J. B. Tatum, “The interpretation of intensities in diatomic molecular spectra”, *Astrophys. J. Suppl. Ser.* 14 (1967) 21

11. J. Thiebaud, S. Crunaire, and C. Fittschen, “Measurements of line strengths in the $2\nu_1$ band of the HO_2 radical using laser photolysis / continuous wave cavity ring-down spectroscopy (CW-CRDS),” *The Journal of Physical Chemistry A* 111 (2007) 6959

12. J.D. DeSain, A.D. Ho, and C.A. Taatjes, “High-resolution diode laser absorption spectroscopy of the O–H stretch overtone band (2,0,0) ⟵(0,0,0) of the HO_2 radical”, *Journal of Molecular Spectroscopy* 219 (2003) 163

13. N.A. Popov "Vibrational kinetics of electronically-excited $N_2(A^3\Sigma,v)$ molecules in nitrogen discharge plasma", *J. Phys. D: Appl. Phys.* 46 (2013) 355204

14. W.H. Wurster, C.E. Treanor, and M.J. Williams, “Non-equilibrium Radiation from Shock-Heated Air”, Final Report. U.S. Army Research Office, Contract No. DAAL03-88K-0174, July 1991, Calspan UB Research Center, Buffalo, NY

15. J. T. Herron, “Evaluated Chemical Kinetics Data for Reactions of $N(^2D)$, $N(^2P)$, and $N_2(A^3\Sigma_u^+)$ in the Gas Phase”, *J. Phys. Chem. Ref. Data* 28 (1999) 1453

16. I. Shkurenkov, D. Burnette, W.R. Lempert, and I.V. Adamovich, “Kinetics of Excited States and Radicals in a Nanosecond Pulse Discharge and Afterglow in Nitrogen and Air”, *Plasma Sources Sci. Technol.* 23 (2014) 065003

17. W. van Gaens, PJ. Bruggeman, and A. Bogaerts, “Numerical analysis of the NO and O generation mechanism in a needle-type plasma jet”, *New J. Phys.* 16 (2014) 063054

18. Y. Ju and W. Sun, “Plasma assisted combustion: Dynamics and chemistry”, *Progress in Energy and Combustion Science* 48 (2015) 21

19. Z. Yin, I.V. Adamovich, and W.R. Lempert, “OH Radical and Temperature Measurements During Ignition of H_2-Air Mixtures Excited by a Repetitively Pulsed Nanosecond Discharge”, *Proceedings of the Combustion Institute* 34 (2013) 3249

20. Z. Yin, A. Montello, C. D. Carter, W. R. Lempert, and I. V. Adamovich, “Measurements of temperature and hydroxyl radical generation/decay in lean fuel–air mixtures excited by a repetitively pulsed nanosecond discharge”, *Combustion and Flame* 160 (2013) 1594